Shape Optimization Based on Parameters from Lifetime Prediction

Bernd Ilzhöfer[1], Ottmar Müller[1], Pascal Häußler[1], Dieter Emmrich[1], Peter Allinger[2]

[1] Institut für Maschinenkonstruktionslehre und Kraftfahrzeugbau,
Universität Karlsruhe (TH)
Kaiserstrasse 12, 76128 Karlsruhe, Germany

[2] FE-Design GmbH
Haid-und-Neu-Strasse 7, 76131 Karlsruhe, Germany

Summary:

In this paper the coupling of conventional structural analysis, methods for lifetime prediction and structural optimization is shown. The objective is an automated shape optimization of machine design components considering the lifetime behavior of the material and the load time history of the load cases.
In the following the realization of the coupling of these methods is presented. As well the difference to conventional "stress optimization" is shown applying the new methods to real world applications.

Keywords:

lifetime prediction, lifetime estimation, optimization, structural analysis, shape optimization

1 Introduction

Usually the dimensioning of structural components with FEA is done with the evaluation of stresses and strains. These measures are compared with reference values which allow an estimate of the lifetime performance of the component [2].

More and more the shape optimization is used to increase the component's lifetime. With this methods the shape is varied in a manner, that an objective function is minimized or maximized under the consideration of further conditions. The variation of the shape is managed by displacing the FEA-nodes. In most cases stress measures are used (e.g. equivalent stresses). By reducing the stresses and strains an enhancement of the lifetime follows indirectly [1]. The disadvantage of this method is that neither the load time history nor the fatigue behavior of the material can be considered within an optimization.

To improve the component's lifetime also the use of lifetime estimation methods is increasing. Using this methods a postprocessing based on local strains is done. Based on this results an assessment and the comparison of different development stages is possible. This methods consider either the load time history of different load cases or the fatigue behavior of the material.

The CAE/Optimization Group of the Institute of Machine Design of the University of Karlsruhe (TH) is working in the field of shape and topology optimization for a couple of years [1], [6], [7]. The team is cooperating and developing with FE-Design GmbH (Karlsruhe). This company is responsible for the program CAOSS which is behind MSC.Construct sold by MSC.Software.

In this context the above described methods (structural analysis, lifetime estimation and optimization) are coupled. Now it is possible to regard the load time history as well as the fatigue behavior of the material during the shape optimization. Because of the fatigue estimation it is now possible to consider constraints that result from the manufacturing process like surface roughness within the optimization.

In the following the realization of the coupling of these methods is shown. As well the difference to common "stress optimization" is described with application examples.

2 Realization of the Shape Optimization Based on Lifetime Prediction Measures

2.1 Objective

The objective of this work is to introduce a method improving the lifetime of machine components by modifying their shape. As mentioned in the introduction this is realized with a coupling of the following methods to run automated structural optimizations:

- Finite Element Method (FEA) for linear static analysis
- Lifetime Prediction as a postprocessing based on the FE-Results
- Shape Optimization of the analyzed component

In this context the term "lifetime prediction" is used for the so called crack initiation time. The total lifetime is the sum of the crack initiation time and the crack propagation time.

2.2 Method, Requirements and Data Flow

The method to realize the aim of a lifetime based shape optimization is to complement a conventional shape optimization process (Figure 1 ,left) with a lifetime prediction tool (Figure 1, right).

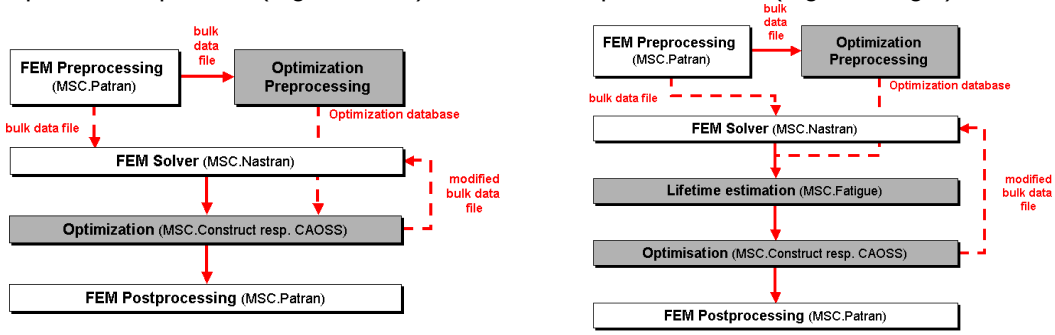

Figure 1 Left: Conventional optimization; right: optimization complemented with a lifetime prediction tool

The requirements are:

- A FEA preprocessor for modeling the problem as well as for preparing the lifetime estimation and the optimization. For the presented work **MSC.Patran** was used.
- A FEA code: In this case **MSC.Nastran**
- A structural optimization program: **MSC.Construct**, respectively **CAOSS** as developed by the authors.

The whole run of all software products is controlled from a bundle of UNIX shell scripts which are collected under the name **mkl/SYSLIFE. mkl/SYSLIFE** uses the scripts (see also Figure 2):

- **syslife_inf**: Initialization file where the global settings are defined (e.g. working directory, paths)
- **syslife**: Prepares the optimization: Here the MSC.Nastran bulk data file is modified, a MSC.Patran session file (setup.ses) is written to control the fatigue processor and the MSC.Construct prepare run is started
- **syslife_opt**: is called from MSC.Construct after the MSC.Nastran run. **syslife_opt** controls the lifetime estimation process

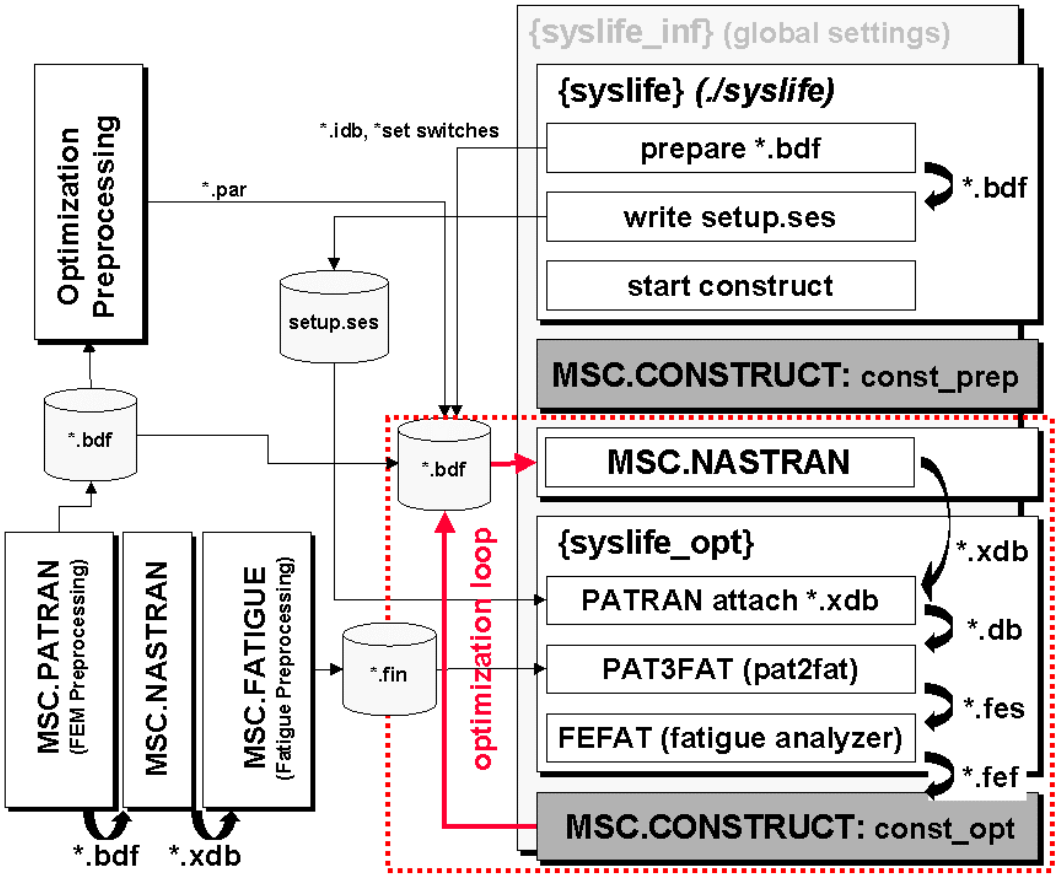

Figure 2: Data flow of the optimization process

To setup up the fatigue based optimization the structure needs to be modeled and analyzed first (see Figure 2, bottom, left side). With this data the job setup of the fatigue analysis can be done resulting in an job information file (*.fin). As well the optimization preprocessing is required. The optimization parameter file (*.par) and MSC.Nastran's bulk data deck (*.bdf) are summarized in an all-in-one-bulk data file (*.bdf).

Calling the script **syslife**, the bulk data file is adapted for the lifetime optimization with further information (Figure 2 top, right side). From **syslife** also a MSC.Patran session file is written. This file attaches the current FE-results to a temporary MSC.Patran database during the optimization loop. Afterwards MSC.Construct is started.

MSC.Construct starts with a first MSC.Nastran run. Then the **syslife_opt** script is executed. The results of the FE-run and the Fatigue job information (*.fin) obtained from the preprocessing are linked together. After this, MSC.Fatigue is able to generate a fatigue information file (*.fes), which is the preparation to execute the lifetime estimation. The MSC.Fatigue results (*.fef) are used as an input for the optimization with MSC.Construct. From MSC.Construct a new bulk date file is created containing the modified geometry. Afterwards a subsequent MSC.Nastran run closes the optimization loop. This loop is run until convergence is achieved.

3 Application Example 1: Moment Loaded Round Bar

On the basis of a moment loaded bar the differences between a conventional optimization based on equivalence stresses [9], and an optimization based on measures of a lifetime estimation are presented.

3.1 Modeling

The bar shown in Figure 3 (length=20mm, diameter=4mm) is modeled with 16,000 3d solid elements. It is fixed on side A at the middle node in all degrees of freedom. The rest of the nodes on that surface are fixed in circumferential direction and in z (all nodes are given in a cylindrical coordinate system).

The bar is loaded at the reference node on side B. This node is coupled via an RBE2-element in all degrees of freedom with the corresponding surface nodes.

The model was generated with MSC.Patran V9. The linear static analysis (Sol101) runs with NASTRAN V70.7 on an HP J5600.

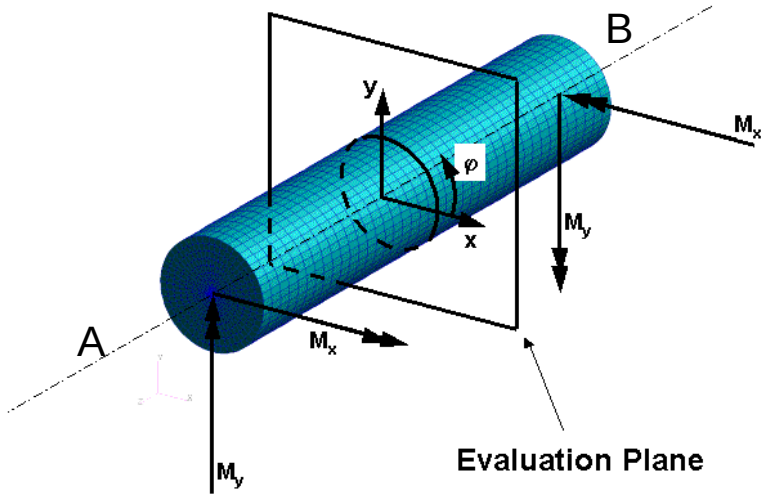

Figure 3: FE-model of the bar

3.2 Loads and materials

3.2.1 FE-Behavior

The constraints are described in chapter 3.1. The bar itself is loaded with two load cases, each with M_x, M_y=2 Nm.

To describe the elasticity of the material (Steel: St 52) the Young's Modulus is set to E = 210,000 MPa and the Poisson ratio to ν=0.3.

Neglecting the shear forces, the following analytical equation holds:

$$\sigma_{z,\max} = \frac{M_{x,y}}{W_{x,y}} = 316MPa$$

The FE-analysis results in $\sigma_{z,max}$=319 MPa, sufficiently far away from the fixture. So that the plausibility is given.

3.2.2 Fatigue behavior

To consider the load time history of the two loads, a sine oscillation is supposed (see Figure 4). For the moment M_x a frequency of f = 10 Hz is assumed, for the moment M_y f = 1 Hz. The load time history scales the given loads.

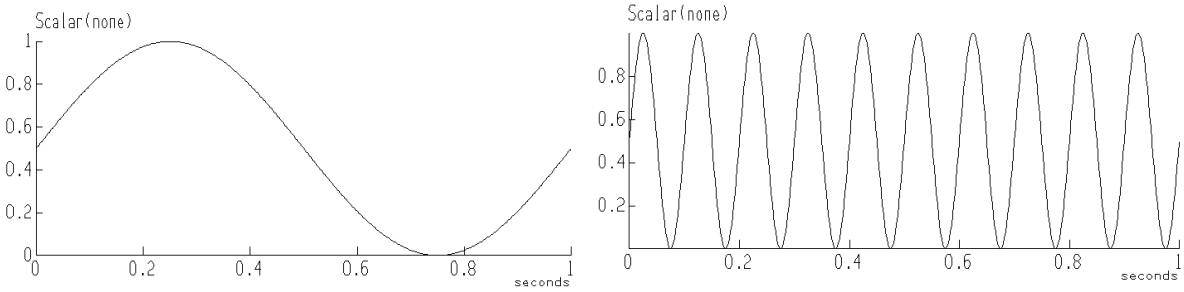

Figure 4: Load time history for the loads M_y (left) and M_x (right)

The material used in this example is a St52 (BS4360-50D) with the material parameters shown in Table 1 and a lifetime behavior represented in Figure 5.

Yield Strength	$R_{p0,2}$	=	355MPa
Ultimate Tensile Strenght	R_m	=	510Mpa
Fatigue Limit	s_{BW}	=	255MPa
Young's Modulus	E	=	210,000MPa
Poisson's Ratio	ν	=	0.3

Table 1: Material parameters of the St52

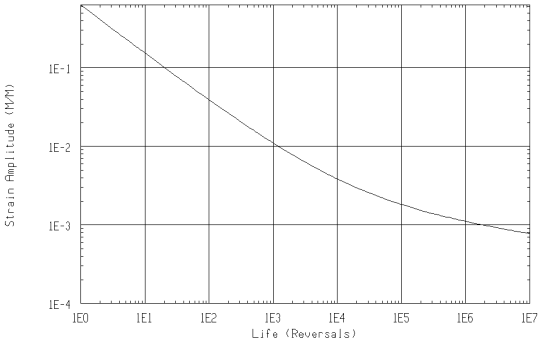

Figure 5: Strain life curve of the St52

3.3 Lifetime Estimation

As analysis type the crack initiation method is chosen [5], [8]. Within the lifetime calculation local strains (maximum absolute principle strains) which are calculated from nodal results are used. Neither surface finishing nor any surface treatments are considered in the calculation. As plasticity correction the method of Neuber is used.

To regard the influence of the mean stresses the base line of the strain life curve is modified by the Smith-Watson-Topper mean stress correction. This method is recommend from MSC.Fatigue for loading sequences where tensile stresses dominate. The Smith-Watson-Topper mean stress correction neglects compression stresses during the damage calculation if the maximum stress becomes zero or negative [3], [5].

3.4 Optimization

The nodes on the circumference of the bar represent the optimization area. A mesh smoothing of all elements is allowed after each iteration step. But all nodes are fixed along the bar-axis. As a further boundary condition a constant volume during optimization is chosen. To have a comparability between the different optimization criteria CAOSS determines the objective value itself. This means that the aim of the optimization is the homogenization of the optimization criteria. After 10 iterations the optimization finishes.

The following optimization criteria are examined:

- Log of damage from a lifetime estimation (lifetime optimization):
  MSC.Fatigue assumes the minimal damage to be 1E-20. To obtain positive optimization values the log of damage is added to 20 (optimization range: $0<\sigma_V<20$):

$$\sigma_V = \log(D) + 20 = \log\left(\frac{1}{N}\right) + 20$$

- von Mises Stress Hypothesis:

$$\sigma_V = \frac{1}{\sqrt{2}}\sqrt{(\sigma_1-\sigma_2)^2+(\sigma_2-\sigma_3)^2+(\sigma_3-\sigma_1)^2}$$

- Normal Stresses Hypothesis:

$$\sigma_V = \max(\sigma_1, \sigma_2, \sigma_3)$$

- Logarithmic Strain Hypothesis (Kuhn/Sauter):

$$b^{S_1-\nu(S_2+S_3)} + b^{S_2-\nu(S_1+S_3)} + b^{S_3-\nu(S_1+S_2)} = b + 2b^{-\nu}, \text{ with } b = \left[\frac{1-\nu}{\nu}\right]^{\frac{1}{1+\nu}} \text{ and } S_i = \frac{\sigma_i}{\sigma_v}$$

3.5 Results

Subsequently the results of the optimization with the different criteria are shown.

3.5.1 Lifetime optimization

Here the logarithmic value of the damage resulting from the lifetime estimation gives the optimization value. Figure 6 shows the damage at the circumference at the evaluation plane (see also Figure 3).

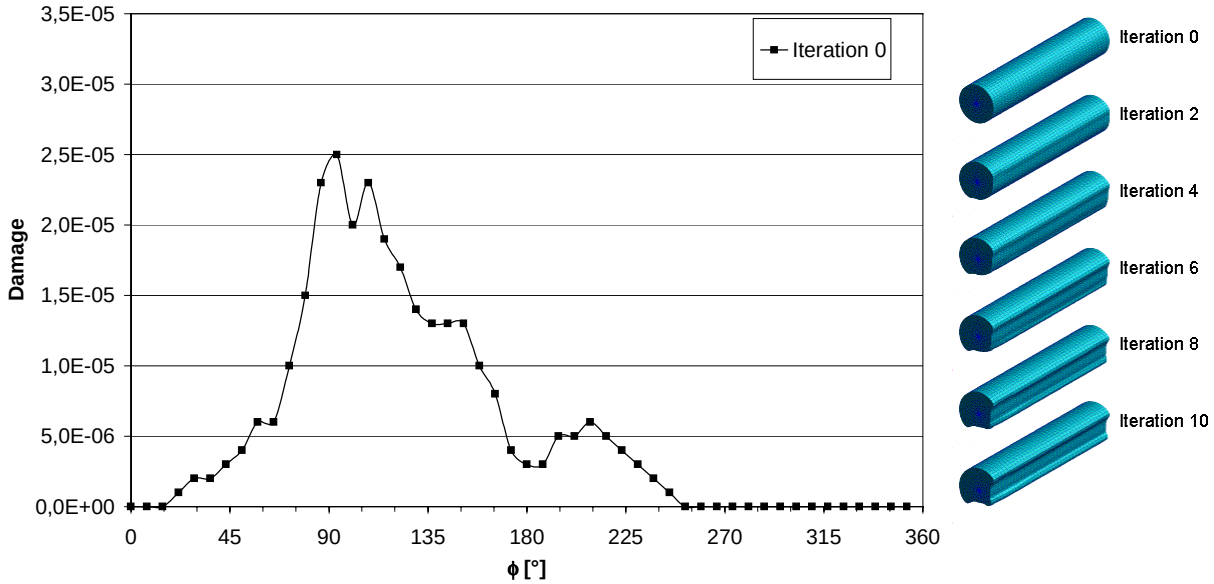

Figure 6: Left: Damage along the circumference in the evaluation plane.
Right: Shape of the bar at different optimization iterations

Dividing the circumference in 90°-ranges (0-90°, 90°-180°, 180°-270°, 270°-360°) the stresses and corresponding damage, represented in Table 2, occur. Remember, that the Smith-Watson-Topper mean stress correction neglects compression stresses and that the frequency of M_x is 10 times higher than the frequency of M_y.

	M_x (f=10Hz)	M_y (f=1Hz)	Effect on damage
0-90°	Tensile stress	Compression stress	↑↑
90°-180°	Tensile stress	Tensile stress	↑↑↑
180°-270°	Compression stress	Tensile stress	↑
270°-360°	Compression stress	Compression stress	-

Table 2: Stresses, induced by the moments and their effect on the damage in 90°-ranges (↑ little effect on damage, ↑↑ effect on damage, ↑↑↑ high effect on damage)

Bearing Table 2 in mind, the diagram in Figure 6 can be explained. At 90° the maximum tensile stress, as a result of M_x occurs. Thus the damage rises from 0° with increasing tensile stresses to the maximum. The neighborhood of 90° must be the region with the most damage caused by the 10Hz-frequence load. Then the damage is decreasing until reaching 180°. That is the region of the maximum tensile stress of M_y. The absolute maximum principle tensile stresses, which are responsible for the damage, have a local maximum at 210°, due to the superposition of the compression stresses of M_x and the tensile stress of M_y. This is the reason why a second local maximum of damage exists.

Because of the run of the curve in the diagram (Figure 6) an an expansion of the shape in the range between 45° and 225° degrees can be expected. A shrinking is supposed in the other regions. This

assumption is proven in Figure 6 on the right side and particularly in Figure 7. In Figure 6 (right) the different shapes after certain optimization iterations are represented. In Figure 7 the development of the shape in the evaluation plane (left) as well as the development of the damage during the optimization is shown. Because of the homogenization process during the optimization a third maximum of damage appears at 315° with the second iteration. The modification of the shape with increasing number of iterations leads to tensile stresses in this region which increase the damage.

As shown in Figure 8 the maximum damage falls by 16% over 10 iterations. Thus the lifetime improvement is 16%.

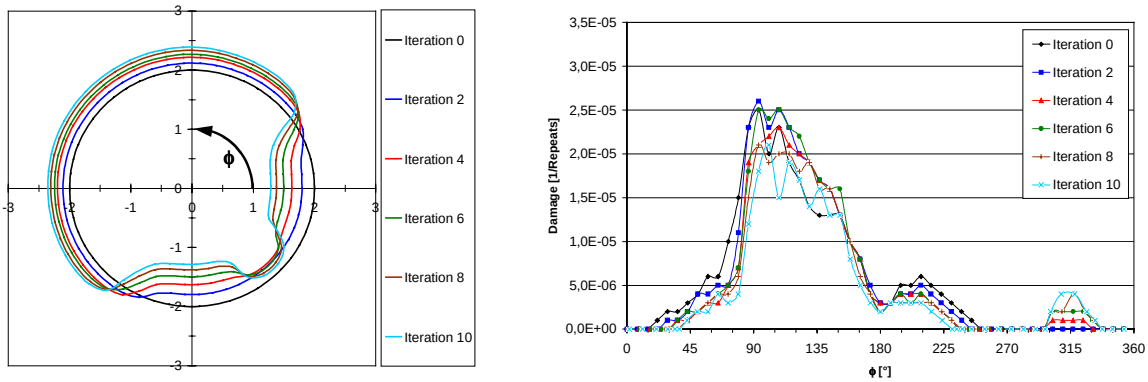

Figure 7: Development of the shape in the evaluation plane (left side) and the effect on the damage along the circumference after different iterations (right side). Objective value: Damage

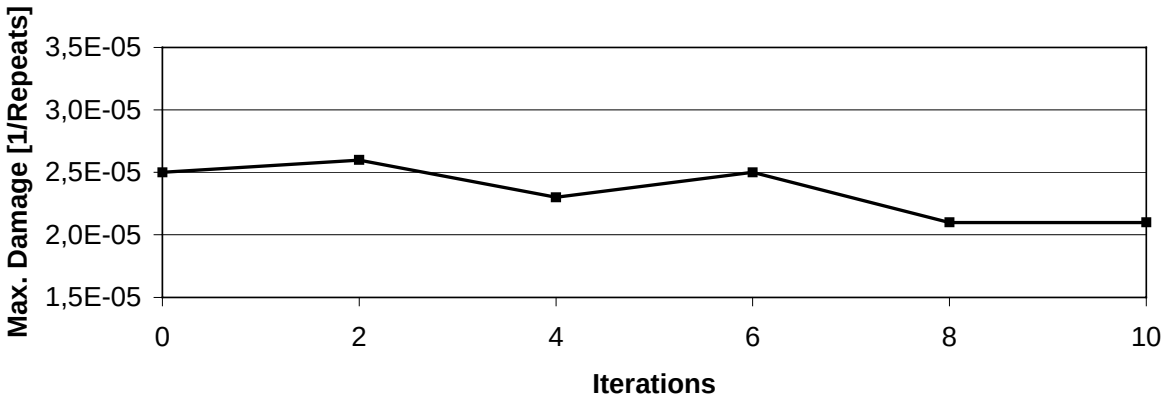

Figure 8: Development of the maximum damage during the optimization process. Objective value: Damage

3.5.2 Optimization with the Von Mises Stress Hypothesis

In Figure 9 (left) the optimization object value, calculated with the von Mises Stress Hypothesis, at the circumference is represented for the basic model (Iteration 0). Because of the maxima in 0°, 90°, 180°, 270° and 360° it can be expected, that the during the optimization the component will grow in those directions. To keep the constant volume, the component has to shrink in the directions of the local minimums (45°, 135°, 225°, 315°). On the right side you can see the development of the bar during the optimization process in the expected manner.

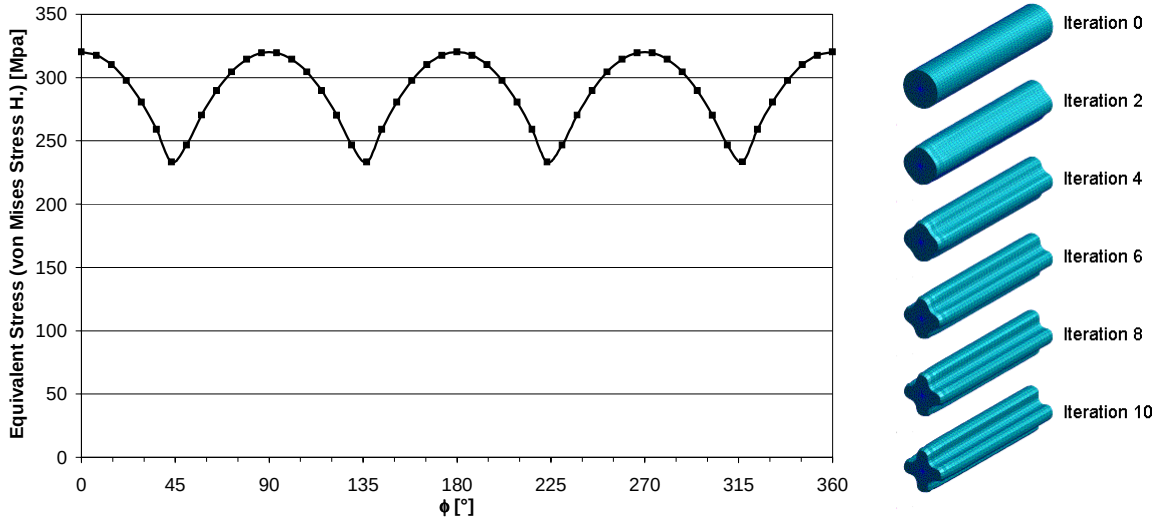

Figure 9: Left: Von Mises stresses along the circumference in the evaluation plane
Right: Shape of the bar at different optimization iterations

In Figure 10 (left) the development of the bar's cross section during the optimization is displayed. On the right side the damages for the iterations at the circumference are shown. In spite of the growth of the shape at 0°; 90°, 180° and 270° the damage is increasing (Figure 11). The reason is that the section modulus is decreasing slightly because of the constant volume over the iterations. With the increasing damage the lifetime is reduced by 28%.

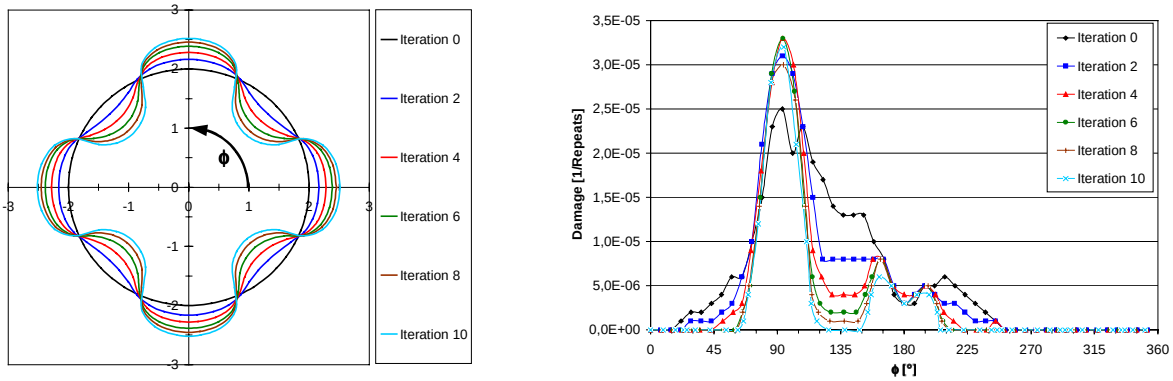

Figure 10: Development of the shape in the evaluation plane (left side) and the effect on the damage along the circumference after different iterations (right side). Objective value: Von Mises Stress Hypothesis

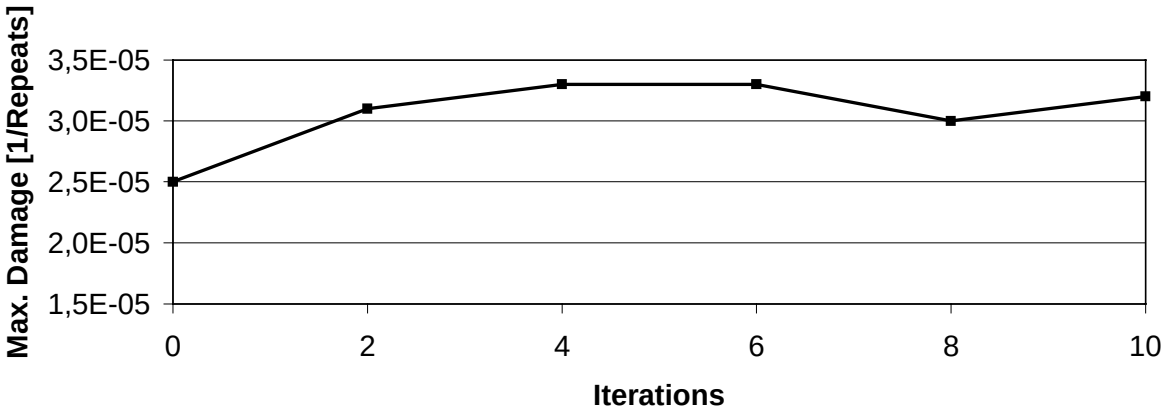

Figure 11: Development of the maximum damage during the optimization process. Objective value: Von Mises Stress Hypothesis

3.5.3 Optimization with the Normal Stress Hypothesis

As shown in Figure 12 two maxima of normal stresses on the circumference exist in the evaluation plane at 90° and 180°. Here, the maximum growth during the optimization process is expected. Between that area a slower growth can be predicted. Because of the zero value of the equivalent stresses between 270° and 360° the component has to shrink in that region to keep the constant volume. The development of the bar's shape during the optimization is shown on the right side of Figure 12.

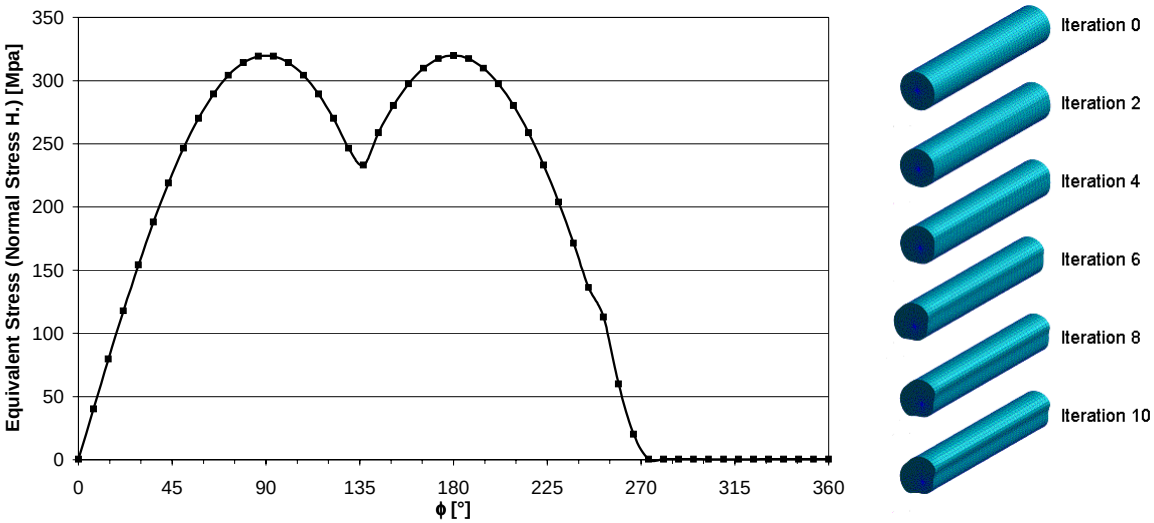

Figure 12: Left: Equivalent stresses (Normal Stress Hypothesis) along the circumference in the evaluation plane. Right: Shape of the bar at different optimization iterations

The development of the shape's cross section and the change of the damage during the optimization is represented in Figure 13. As shown in Figure 14 the damage is increasing during the optimization. Again the reduced section modulus is responsible for that behavior. The increasing damage results in a lifetime reduction of 24%.

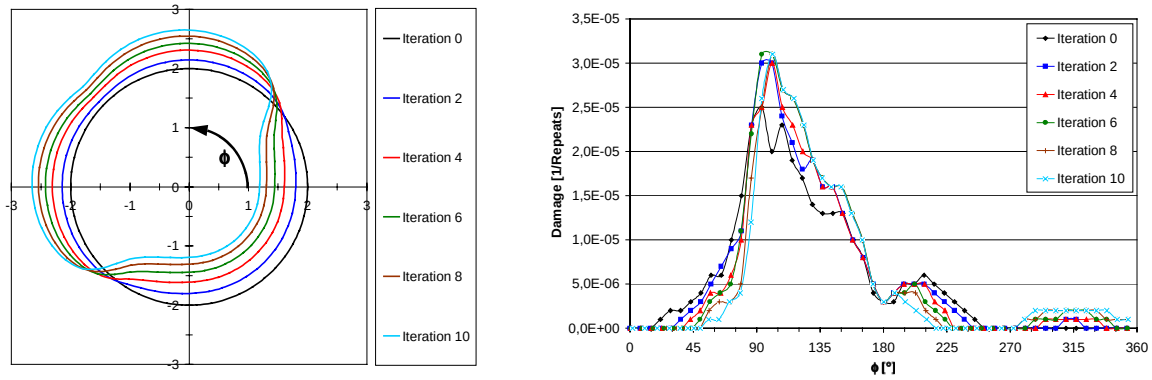

Figure 13: Development of the shape in the evaluation plane (left side) and the effect on the damage along the circumference after different iterations (right side). Objective value: Normal Stress Hypothesis

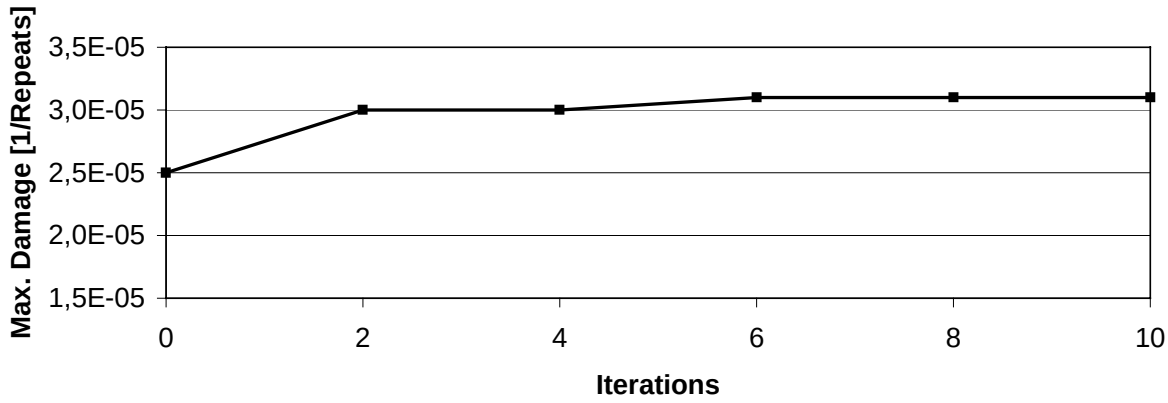

Figure 14: Development of the maximum damage during the optimization process. Objective value: Normal Stress Hypothesis

3.5.4 Optimization with the Logarithmic Strain Hypothesis

The equivalent stress curve at the circumference with the Logarithmic Strain Hypothesis of Kuhn and Sauter (see Figure 15) resembles the stress curve of the Normal Hypothesis. However, the Logarithmic Strain Hypothesis considers compression stresses as well, as seen in the area between 180° and 360°. It is no surprise that during the optimization the shape and the development of the damage show a rather similar behavior to the optimization based on the Normal Stress Hypothesis (Figure 15 and 16).

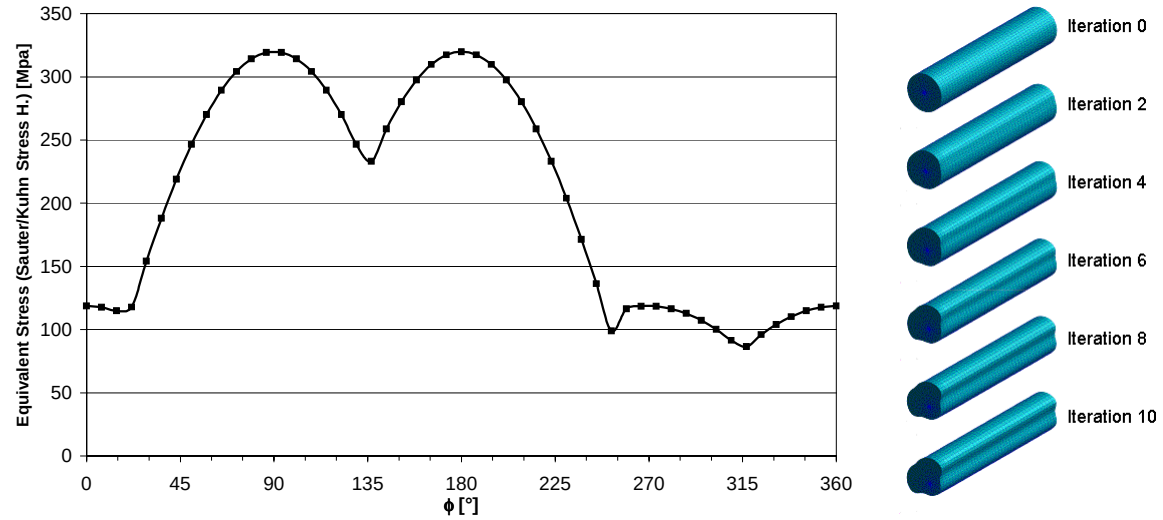

Figure 15: Left: Equivalent stresses (Logarithmic Strain Hypothesis) along the circumference in the evaluation plane. Right: Shape of the bar at different optimization iterations

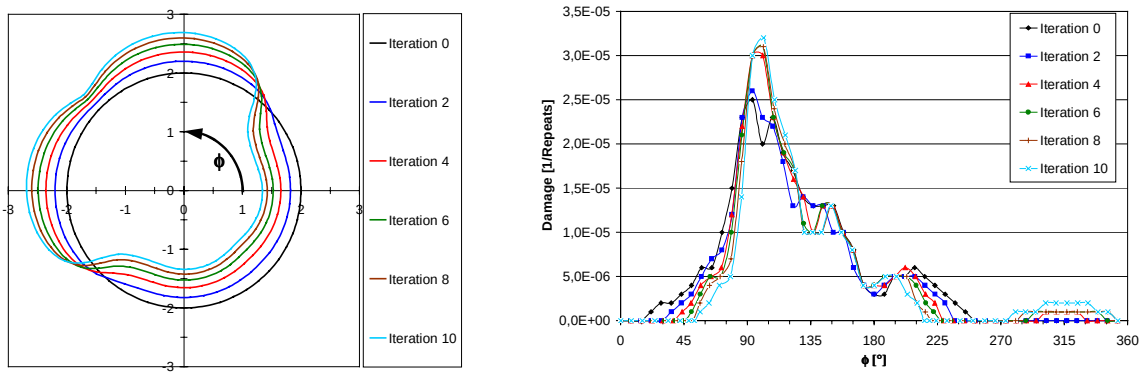

Figure 16: Development of the shape in the evaluation plane (left side) and the effect on the damage along the circumference after different iterations (right side). Objective value: Logarithmic Strain Hypothesis

The same applies for the development of the damage during the optimization, which ends by a 28% reduced lifetime (Figure 17).

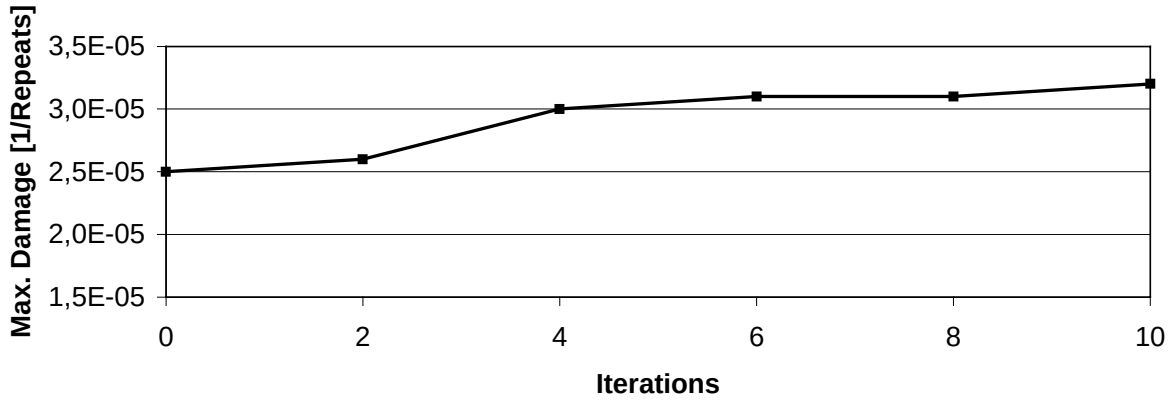

Figure 17: Development of the maximum damage during the optimization process. Objective value: Logarithmic Strain Hypothesis

3.6 Conclusion

With respect to the applied boundary conditions (constant volume), only the optimization based on values of a lifetime prediction gives an improvement in lifetime (Figure 18). Using conventional optimization values, like as equivalent stresses and strains, the damage is increasing and thus the lifetime is decreasing during the optimization.

The choice of the optimization strategy, using different equivalent stresses or the damage as optimization value, has a considerable effect on the optimized shape and thus on the structural and lifetime behavior.

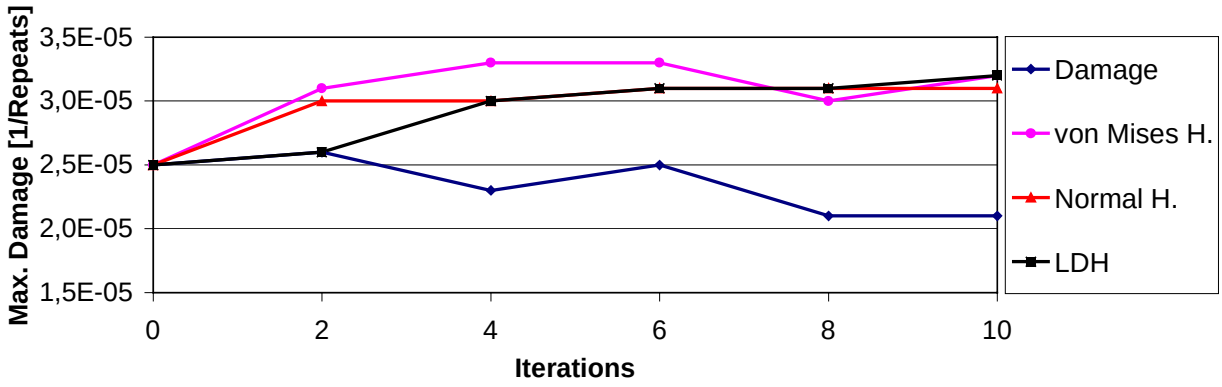

Figure 18: Development of the maximum damage during the optimization process regarding different optimization values (LDH=Logarithmic Strain Hypothesis)

4 Application Example 2: Steering Knuckle

The next example, on the basis of a steering knuckle, shows a further comparison of the optimization with different optimization values [4].

4.1 Modeling

The FE-model of the steering knuckle (Figure 19) consists of approx. 22,000 degrees of freedom. It is fixed in the x-y plane at the brackets of the steering arm and at the suspension arm via fully coupled RBE2-elements. The middle of the strut mount is closed with shell elements (Quad4) which are connected via an RBE2-element with an in all degrees of freedom fixed reference node.

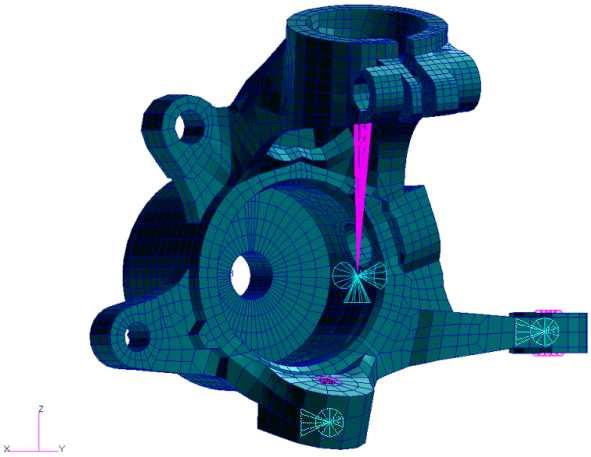

Figure 19: FE-model of the steering knuckle with boundary conditions

4.2 Loads and Materials

4.2.1 FE-Behavior

The constraints are described above. The component is loaded with 3 different load cases (see Figure 20):

- Load case 1: *Straight Driving* (left)
- Load case 2: *Rolling Turn* (middle)
- Load case 3: *Deceleration* (right)

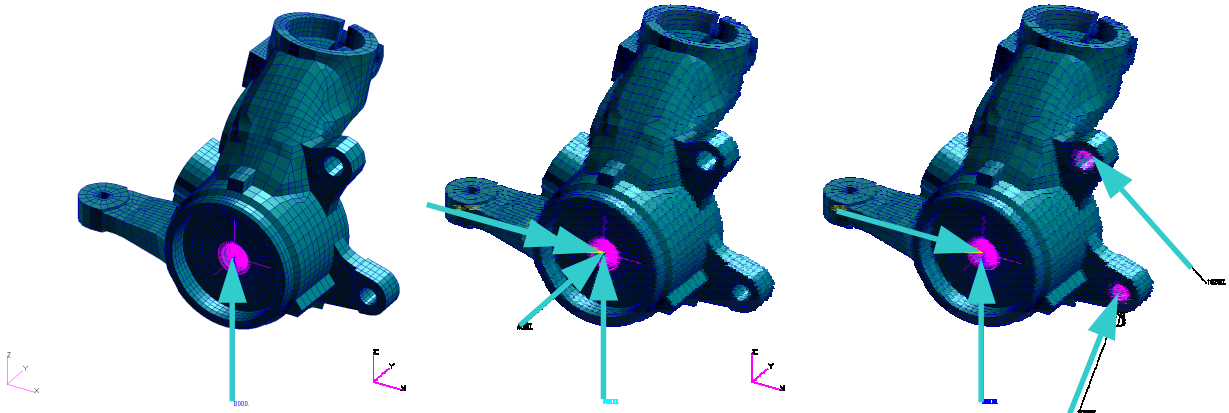

Figure 20: Applied load cases with plotted forces and moments (left: *straight driving*, middle: *rolling turn*, right: *Deceleration*)

The loads of each load case are given in Table 3.

		Straight Driving	*Rolling Turn*	*Deceleration*
Forces and moments at the wheel bearing	Force x	-	-	4,800N
	Force y	-	4,800N	-
	Force z	3,000N	4,800N	4,800N
	Moment x	-	1,877,000Nmm	-
Forces at the break mountings in circumferential direction around the wheel bearing	Force (circumf.)	-	-	10,280N at each bolted joint

Table 3: Loads for each load case

For the example a perlitic cast iron with spheroidal graphite: BS2789 Grade 800, was chosen. To describe the elastic material behavior the Young's Modulus for the FE-analysis is given with E = 162,000 MPa, the Possoin's Ratio with $\nu = 0.3$.

4.2.2 Fatigue Behavior

The loads on the steering knuckle are scaled with the load time histories given in Figure 21. There 20 seconds represent one repeat.

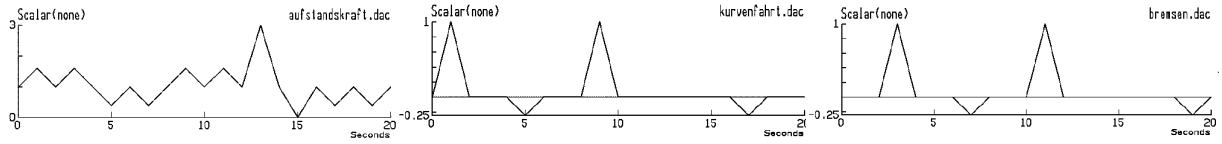

Figure 21: Load time histories of the load cases (left: *straight driving*, middle: *rolling turn*, right: *deceleration*)

In Table 4 the material parameters are given for the BS2789. On the right side you can see the material's strain life curve (figure 22).

Yield Strength	$R_{p0,2}$	=	355MPa
Ultimate Tensile Strenght	R_m	=	510Mpa
Fatigue Limit	s_{BW}	=	255MPa
Young's Modulus	E	=	162,000MPa
Poisson's Ratio	ν	=	0.3

Table 4: Material parameters

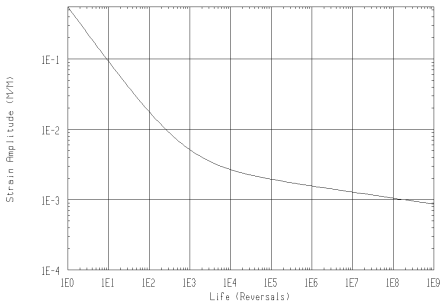

Figure 22: Strain life curve of the used material

4.3 Lifetime Estimation

The optimization area and thus the area used for the lifetime estimation is highlighted in Figure 23. This area is chosen because it is assumed to be the area which may be modified in the further evolution process of the component. The following requirements are applied for the lifetime estimation:

- Crack initiation method
- Analysis on local maximum absolute principle strains
- Neuber's Plasticity correction
- Mean stress correction with the Smith-Watson-Topper Method

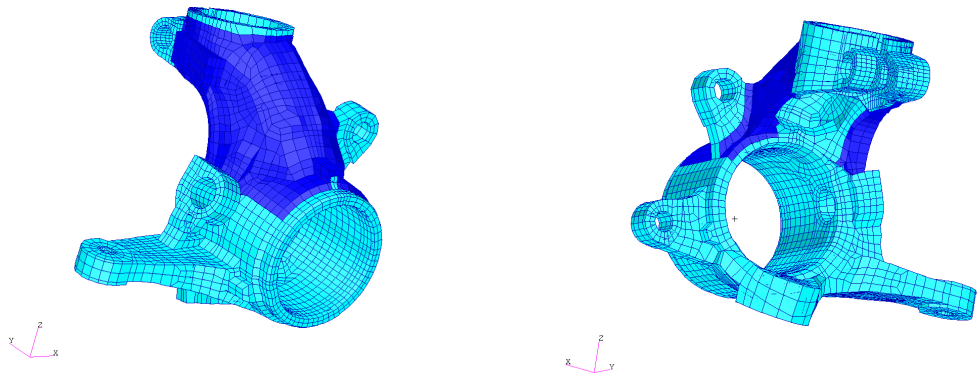

Figure 23: Optimization region

4.4 Optimization

As mentioned above, the optimization area is identically with the region for which the lifetime is estimated (see Figure 23). During the optimization the volume is kept constant again. The optimizer (CAOSS) determines the objective value by itself. No mesh smoothing is allowed. The optimization stops after 10 iterations.

The optimization is carried out with following criteria:

- Logarithmic values of the damage
- Life in Repeats
- Equivalent stresses resulting from the Normal Stress Hypothesis
- Equivalent stresses resulting from the von Mises Stress Hypothesis

4.5 Results

In Figure 24, the von Mises stress distributions of the 3 load cases are represented. In each load case the maximum stresses occurs in the ribs of the strut mount because of the perpendicular forces (in z direction), causing a bending moment within the ribs. The load case *deceleration* is the worst, because of the moment supported by the steering arm, due to the braking forces applied at the brake mounting.

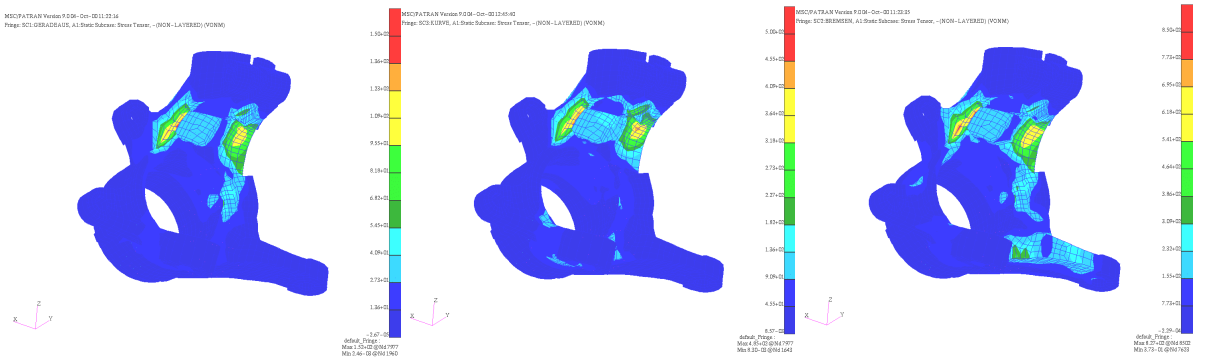

Figure 24: Von Mises stress distribution for the load cases (left: *straight driving*, middle: *rolling turn*, right: *deceleration*)

Because of the FE-results, the lowest lifetime can be expected within the rips of the strut mount. This assumption is proven with the lifetime distribution of the steering knuckle in Figure 25. The minimum of the lifetime is given with only 1,761 calculated repeats.

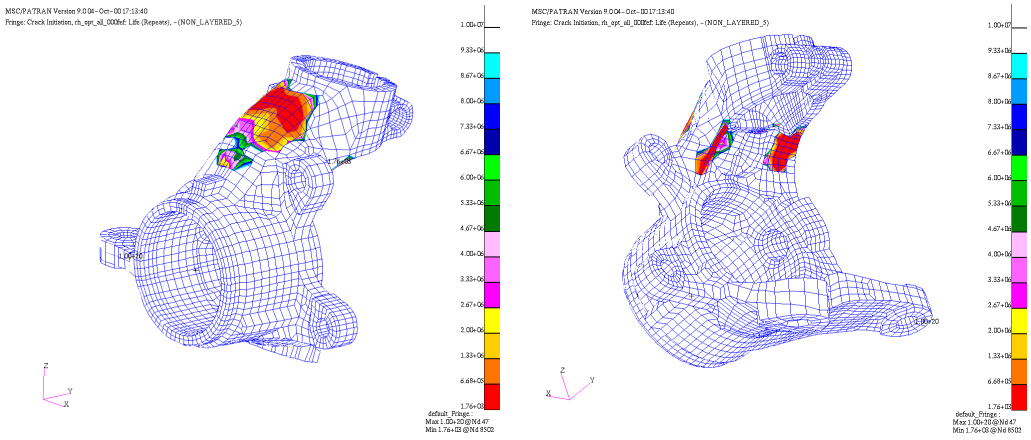

Figure 25: Damage distribution of the steering knuckle (basic model)

With a log of the damage as chosen reference value, the maximum lifetime improvement is approx. 2.5 times (see Figure 26). The reason for this little improvement is that the objective values are between 0 and 20. Thus the gradient to the local maximum is very low. Contrary to this, the optimization with repeats as objective values, give a high gradient to the local minimum. The homogenization of the lifetime induces very fast modifications of the area with the local minimum. The improvement shows a factor of approx. 5,000. The optimization stops after the 5th iteration because of warped elements.

Between both extremes, the conventional optimization with equivalent stresses as objective values can be found. Because of the consideration of the compression stresses, the von Mises stress level is higher than that with equivalent stresses resulting from the Normal Stress Hypothesis. This is probably the reason, why the optimization with von Mises stresses is slightly faster and shows a higher improvement (lifetime improvement: 28 times) compared with the optimization used the Normal Stress Hypothesis (lifetime improvement: 16 times).

The large difference between the several optimization methods shows that a calculation of new equivalence stresses on the basis of lifetime values is desirable (considering the stress-life curve). This way, the optimization values of the different methods resemble the same order of magnitude. Hence the controller behavior of the optimizer will be similar. With this the comparison among the optimization with lifetime values and equivalent stresses will be improved.

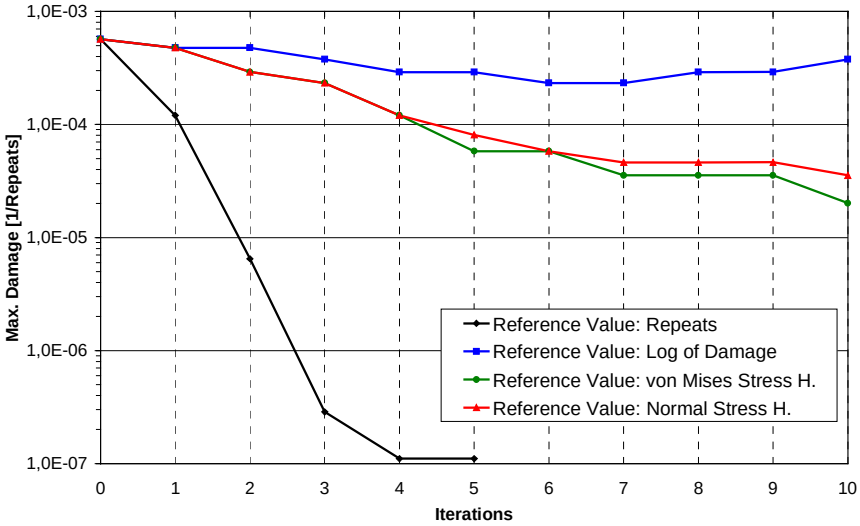

Figure 26: Maximum damage in the optimization area during the optimization

5 Conclusion

The presented paper shows the realization of a an automated shape optimization process with optimization values from a life time prediction compared with conventional optimizations on equivalent stresses.

With the first example, a moment loaded round bar, the different optimization strategies show remarkable differences in the optimized shape as well as in the analyzed lifetime. With the optimization on equivalent stresses, the estimated life time is even reduced. Whereas the optimization with damages as optimization values shows an improvement in lifetime.

The optimization of a steering knuckle points out the large influence of the chosen optimization criterion on the optimization result. The optimization of lifetime repeats shows a very fast improvement of the lifetime, because of the high gradient of the component's lifetime. On the other hand the optimization with logarithmic values of the damage is very slow, because of the low gradient. The optimization speed of a conventional optimization with equivalent stresses (Normal Stress Hypothesis, von Mises Stress Hypothesis) is between the above described strategies.

To improve the comparability between the different methods, it would be desirable to calculate an equivalence stress on the basis of lifetime values, which will be subject of further studies.

Summarizing, the advantage of the optimization on values from a lifetime estimation are:

- Considering the load time history during the optimization
- Load cases with a high damage quota are considered in an adequate manner during the optimization
- With the optimization process based on lifetime estimation, surface conditions (surface treatment, -roughness etc.) can be considered during the optimization

6 Acknowledgement

The Deutsche Forschungsgemeinschaft (DFG) has financially supported the presented study in the Collaborative Research Center SFB 483, Project C5. The support is gratefully acknowledged.

7 References

[1] Allinger, P.; Bakhtary, N.; Friedrich, M.; Müller, O.; Mulfinger, F.; Puchinger, M.; Sauter, J.: “A New Approach for Sizing, Shape and Topology Optimization”, SAE Congress, Paper-No. 960814, 1996

[2] Haibach, E.: „Betriebsfeste Bauteile“, Springer-Verlag: Berlin, 1992

[3] Leese, G. E.: „Multiaxial Fatigue: Analysis and Experiments“, AE14, 1989, pp. 107-119

[4] MSC.Fatigue: „QuickStart Guide”, 1998, pp. 11-1–11-18

[5] MSC.Fatigue: “User’s Manual”, Volume2, 1998, pp. 1265-1266

[6] Müller, O.; Allinger, P.; Sauter, J.; Albers, A.: Topology Optimization of Large Real World Structures, NAFEMS World Congress '99 - Newport, Rhode Island, USA, April 25-28, Proceedings ISBN 1-874376-25-5, Volume 2, pp 827-839, 1999.

[7] Müller, O.; Ilzhöfer, B.; Häußler, P.; Albers, A.: Multidisciplinary shape and topology optimization and its integration in the product development process for the effective development of competetive products, ICED 99 12th International Conference on Engineering Design, Munich, August 24-26, Volume 2, pp 655-660, 1999.

[8] Rice, R.C.; Leis, B.N. et al: “Fatigue Design Handbook”, AE10, 2nd Edition, 1988, pp.235-249

[9] Sauter, J.: „Über Festigkeitshypothesen und Wege zur Verifizierung“, Dissertation; Universität Karlsruhe, 1993.